

# Study of the influence of geometric imperfections and residual stresses on the stability of steel columns subjected to axial compression

Mariana Mohana Rodrigues da Silva<sup>1</sup>, Evandro Parente Jr.<sup>1</sup>, Marcelo Silva Medeiros Jr.<sup>1</sup>

<sup>1</sup>*Laboratório de Mecânica Computacional e Visualização, Departamento de Engenharia Estrutural e Construção Civil, Universidade Federal do Ceará  
Campus do Pici, Bloco 728, 60440-900, Fortaleza/CE-Brazil  
marimohana@hotmail.com, evandro@ufc.br, marcelomedeiros@ufc.br*

**Abstract.** Imperfections and residual stresses play a major role in the steel columns' final compressive strength. This research was geared towards assessing the influence of the geometric imperfections and residual stresses on the strength of steel columns subjected to axial compression. For this purpose, computational models of I-beam steel columns were developed and analyzed using the Finite Element Method. Initially, a linearized elastic buckling analysis was carried out to determine the critical loads (eigenvalues) and buckling modes (eigenvectors). Following this, nonlinear analyses were conducted considering materially and geometrically nonlinear effects to evaluate the column's strength considering the geometric imperfections with different amplitudes and the shape of the first buckling mode. The elastoplastic model without hardening was adopted to represent the material nonlinearity. Finally, nonlinear analyses were carried out considering different levels of residual stresses for each geometric imperfection amplitude. The results show that the geometric imperfections and residual stresses have a strong influence on the load carrying capacity steel columns leading to a column curve close to the curve adopted by NBR 8800:2008. Therefore, both geometric imperfections and residual stresses should be properly considered in advanced analysis procedures for steel structures.

**Keywords:** Steel columns, Geometric imperfections, Residual stresses.

## 1 Introduction

Columns are vertical structural elements that support and transmit loads from beams and slabs to the foundation. They are typically subjected to normal compressive stresses, making them prone to instability (buckling). This phenomenon is practically insensitive to the material strength, being related to the stiffness and geometric properties of the structural element [1].

Regarding steel columns, their structural profiles can be classified based on the production process into rolled and welded profiles. Rolled profiles are obtained through the mechanical transformation process (rolling), while welded profiles are created by joining rolled profiles using electric welding. Both processes cause initial geometric imperfections and residual stresses, which reduce the columns final compressive strength and contribute to buckling [2].

Initial geometric imperfections are small irregularities in the geometry of the structural element that are imperceptible to the naked eye. These include initial bends and slight deviations from the ideal perfectly straight geometry [1]. Residual stresses, on the other hand, arise from uneven cooling of the element, where inner sections cool more slowly than outer edges. Over the years, several experimental studies have been conducted to confirm the existence of residual stresses in steel columns. These studies show that the intensity and distribution of residual stresses vary depending on the dimensions, geometry of cross-section, cooling rate, and other variables [2].

To assess the impact of these phenomena on compressive strength, the NBR 8800:2008 standard provides a column design curve. This curve relates the reduction factor due to compressive strength ( $\chi$ ) with the reduced slenderness ratio ( $\lambda_0$ ), both dimensionless parameters [3]. However, the distribution and intensity of residual stresses vary between structures, causing the buckling curve to potentially underestimate or overestimate actual values depending on the specific scenario under review [1].

In this context, the objective of this work is to investigate the influence of initial geometric imperfections and residual stresses on columns final compressive strength. For this purpose, finite element models were developed using the Finite Element Method. These models will simulate the behavior of pinned-end HP 250x85(H) steel

columns subjected to axial compression. The study also includes a detailed comparison with the column curve provided by the NBR 8800:2008.

## 2 Methodology

To simulate the behavior of steel columns subjected to axial compression, eight models were developed using the shell finite elements. All models were based on the HP 250x85(H) hot-rolled section from Gerdau's catalog (Fig. 1) and ASTM A36 steel, which has a yield strength ( $\sigma_y$ ) of 250 MPa. To obtain the columns curves, numerical models of steel columns were developed with different values of slenderness ratio ( $\lambda$ ): 45, 60, 75, 90, 105, 120, 135 and 150.

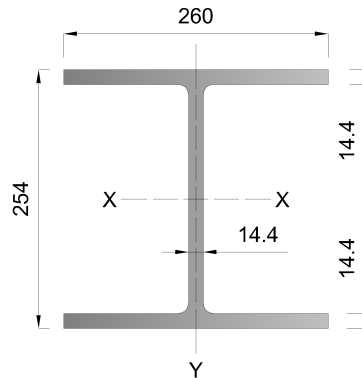


Figure 1. Details of the dimensions of the rolled section in mm

The columns were discretized using four node shell elements based on the Reissner-Mindlin theory. After a mesh convergence study, the best results were found to be with elements of 20 mm in size. The Fig. 2 illustrates the mesh convergence analysis for the  $\lambda=90$  model, with the last two points showing a difference of 0.01%. The pinned-end condition was simulated by creating reference points at the center of the top and bottom ends of the web. At the bottom point, translations were constrained in all directions, while at the top point, translations were restrained only in the  $x$  and  $z$  directions. Rotational movements were allowed at both points in the  $x$  and  $z$  directions (Fig. 3).

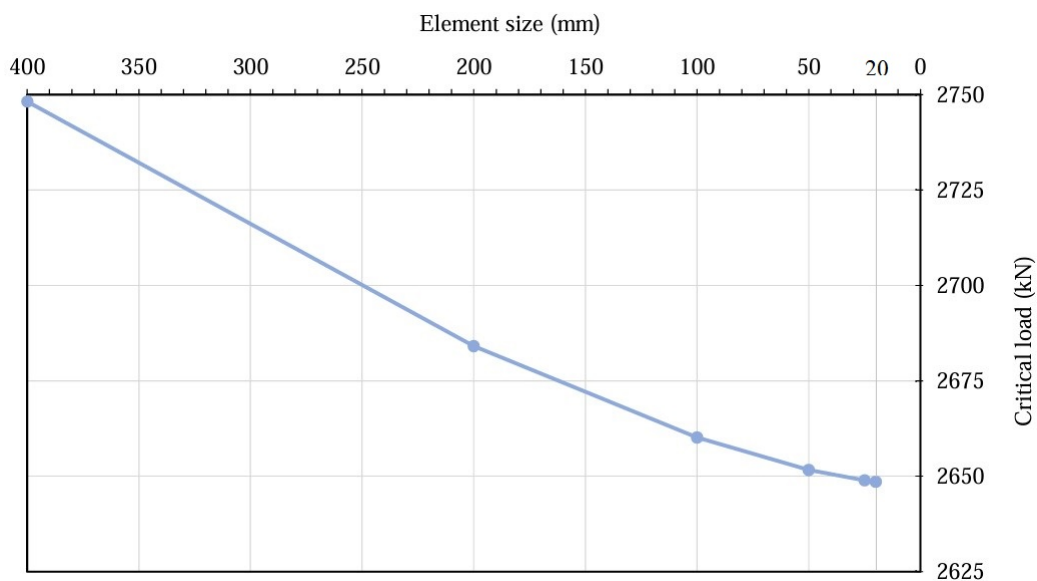


Figure 2. Mesh convergence study

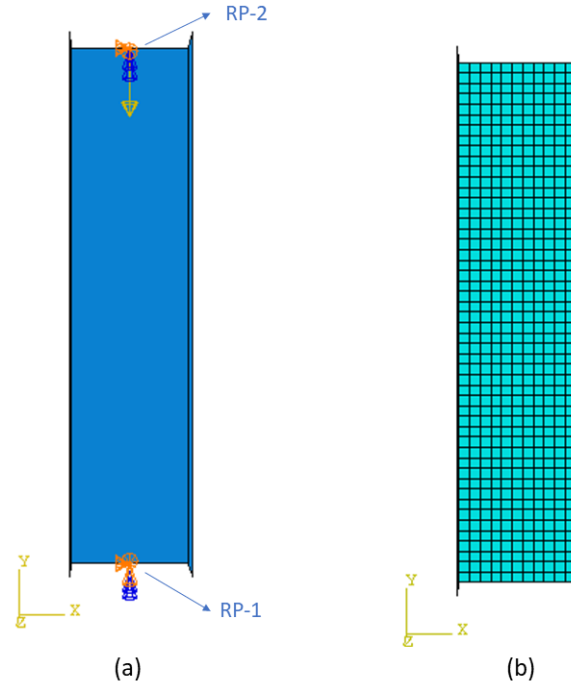


Figure 3. (a) Details of the boundary condition; (b) Details of the finite element mesh

Initially, a linearized elastic buckling analysis was conducted to determine the critical loads (eigenvalues) and the buckling modes (eigenvectors). Additionally, the critical loads provided by the software were compared to the classical Euler buckling load ( $P_{cr}$ ) for pinned-end columns [4]:

$$P_{cr} = \frac{\pi^2 EI}{L^2} \Rightarrow \sigma_{cr} = \frac{P_{cr}}{A} = \frac{\pi^2 E}{\lambda^2}, \quad \lambda = \frac{L}{r} \quad (1)$$

where  $E$  is the elastic modulus,  $A$  is the cross-sectional area,  $I$  is the moment of inertia of the cross-sectional area,  $L$  is the effective length,  $\lambda$  is the slenderness ratio, and  $r = \sqrt{I/A}$  is the radius of gyration of the cross-sectional area.

Euler's formulation is suitable for calculating the critical load of perfect columns. However, in practice, steel structural elements often have initial geometric imperfections and residual stresses from the manufacturing process. These factors reduce the columns final compressive strength and should be properly considered in advanced analyses [4].

To assess the effect of these phenomena, a nonlinear analysis was carried out. Initially, geometric imperfections of  $L/2000$ ,  $L/1500$ ,  $L/1000$  and  $L/500$  were introduced into each model. According to the AISC standard, the maximum fabrication tolerance for a steel column out-of-straightness is  $L/1000$  [5]. Therefore, a geometric imperfection of  $L/1000$  was fixed, and a residual stress ( $\sigma_r$ ) equal to 5%, 10%, 20% and 30% of  $\sigma_y$  was added to each model. In total, 64 analyses were conducted.

Finally, column curves were plotted for the eight models analyzed and compared with the curve specified by NBR 8800:2008 and the Euler curve for ideal columns. Columns with reduced slenderness ratio ( $\lambda_0$ ) less than 1.5 are classified as medium columns. In these cases, failure results from instability and reaching the material's strength limit (inelastic buckling). Columns with  $\lambda_0$  greater than 1.5 are classified as slender columns, failing due to instability (elastic buckling) [1]. The NBR 8800:2008 provides equations for calculating the reduction factor related to compressive strength ( $\chi = \sigma_u/f_y$ ) in both cases:

$$\begin{cases} \lambda_0 \leq 1.5 : & \chi = 0.658\lambda_0^2 \\ \lambda_0 \geq 1.5 : & \frac{0.877}{\lambda_0^2} \end{cases} \quad (2)$$

where  $\lambda_0 = \lambda/\lambda_p$  and  $\lambda_p = \pi\sqrt{E/f_y}$ .

## 2.1 Residual stresses

For I-beam steel columns, the flanges tips tend to cool more rapidly than the intersection between the web and the flange during the rolling process. Thus, the flanges tips cool and contract first, and when the center of the flange cools and tries to contract, the deformation is resisted by the cold and rigid flanges tips. A similar phenomenon occurs in the web center, which cools more rapidly than the web-flange intersection. This results in residual compressive stresses at the flanges tips and web center and residual tension stresses at the flanges center and web-flange intersection [5].

In rolled and welded sections, a linear distribution of residual stresses is typically used to address their variability [6]. This study considered a simplified version of this distribution, illustrated in Fig. 4. Therefore, compressive residual stresses were added at the tips of the flange, while tension stresses were added at the center of the flange. In the same way, tension residual stresses were added at the ends of the web and compressive stresses were added at the center of the web (Fig. 5).

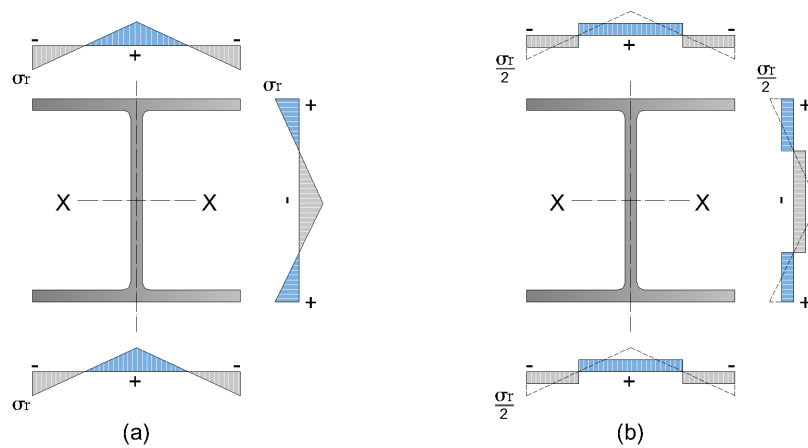


Figure 4. (a) Linear distribution of residual stresses; (b) Approximate distribution applied to the models

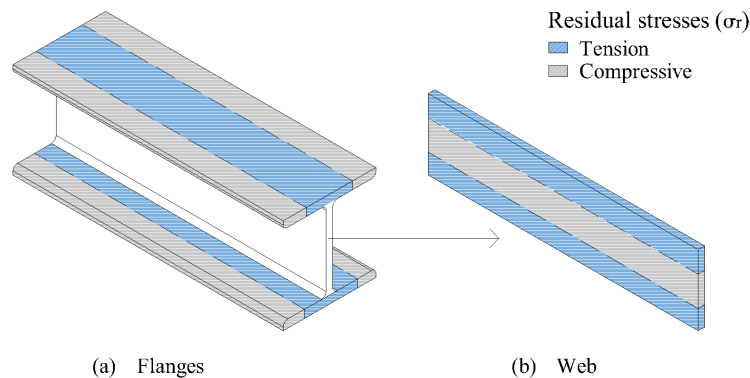


Figure 5. Distribution of residual stresses along the numerical models

Studies have shown that the average value of the maximum residual stress in hot-rolled wide-flange shapes is approximately 30% of  $\sigma_y$  [5]. Therefore, to investigate the reduction in load capacity of steel columns, two curves were constructed correlating axial force ( $P$ ) with lateral displacement. The first curve considers a geometric imperfection of  $L/1000$ , free of residual stresses, while the second curve considers a geometric imperfection of  $L/1000$  with a residual stress of 30%.

## 3 Results and discussion

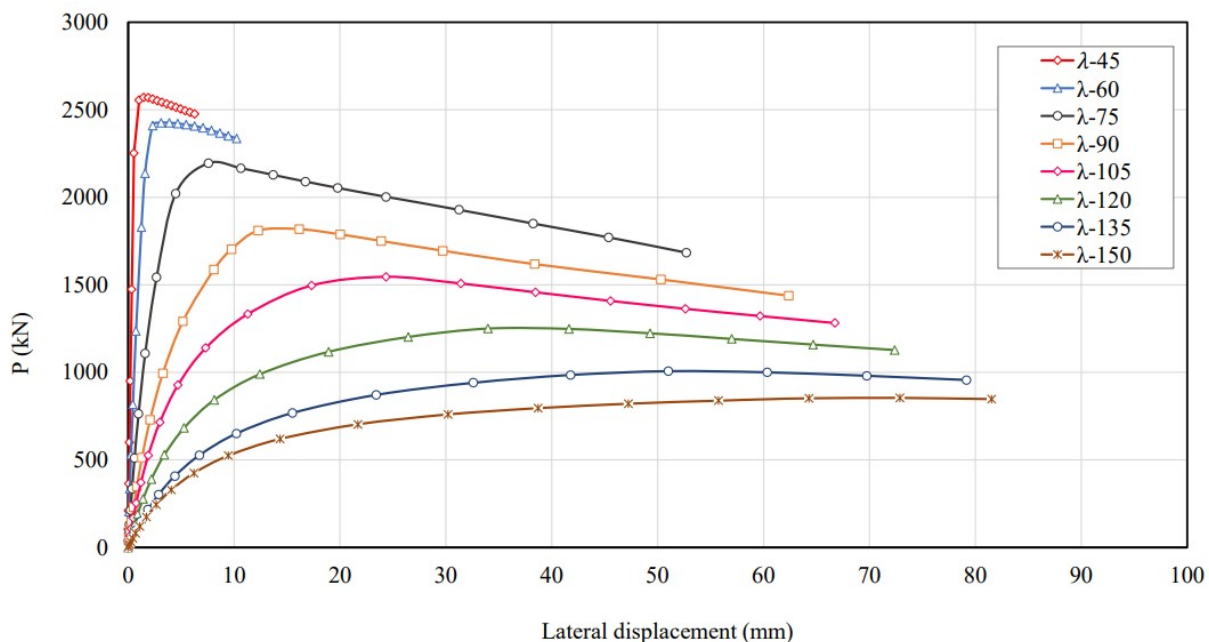
Tab. 1 shows a comparison between critical loads (eigenvalues) obtained from the software and those provided by Euler formulation. As expected, the numerical results for the critical load were lower than those obtained

by the Euler formulation. This occurs because finite element models use Reissner-Mindlin shell elements that incorporate transverse shear and local effects.

Table 1. Linearized buckling loads

Models	$P_{cr_{Num}}$ (kN)	$P_{cr_{Euler}}$ (kN)	Diff. (%)
$\lambda$ -45	10453.2	10637.52	1.73
$\lambda$ -60	5875.47	5930.54	0.93
$\lambda$ -75	3753.45	3775.38	0.58
$\lambda$ -90	2648.58	2659.38	0.41
$\lambda$ -105	1938.15	1943.90	0.30
$\lambda$ -120	1479.29	1482.63	0.23
$\lambda$ -135	1179.82	1181.95	0.18
$\lambda$ -150	952.58	953.97	0.15

Fig. 6 and 7 present the curve with the relationship between axial force ( $P$ ) x lateral displacement for each model. It is observed that initially, all columns show a linear load-displacement relation. However, beyond a certain point, they transition to nonlinear behavior, where the maximum load correspond to a limit point of the equilibrium path. Additionally, columns with lower slenderness ratios ( $\lambda$ ) demonstrate higher load capacity, resulting in a longer linear segment. Furthermore, it is noted that the introduction of residual stress has led to a decrease in the load capacity of all columns. This suggests that the structure now experiences the same displacement for a lower applied load.

Figure 6. Load-displacement relation for models with geometric imperfection of  $L/1000$ , free of residual stresses

The graph in Fig. 8 illustrates the column curve for different initial geometric imperfections. It is evident that geometric imperfections negatively impact the columns final compressive strength. The greater the imperfection, the lower the load required for buckling to occur. Consequently, the lowest critical loads are observed in models with an imperfection of  $L/500$ , while the highest are seen in models with an imperfection of  $L/2000$ . Additionally, as the initial geometric imperfection increases, the column curve deviate further from the curve derived from Euler formulation for perfectly straight columns. The curve that most closely aligns with the one proposed by NBR 8800:2008 is the one with an imperfection of  $L/1000$ .

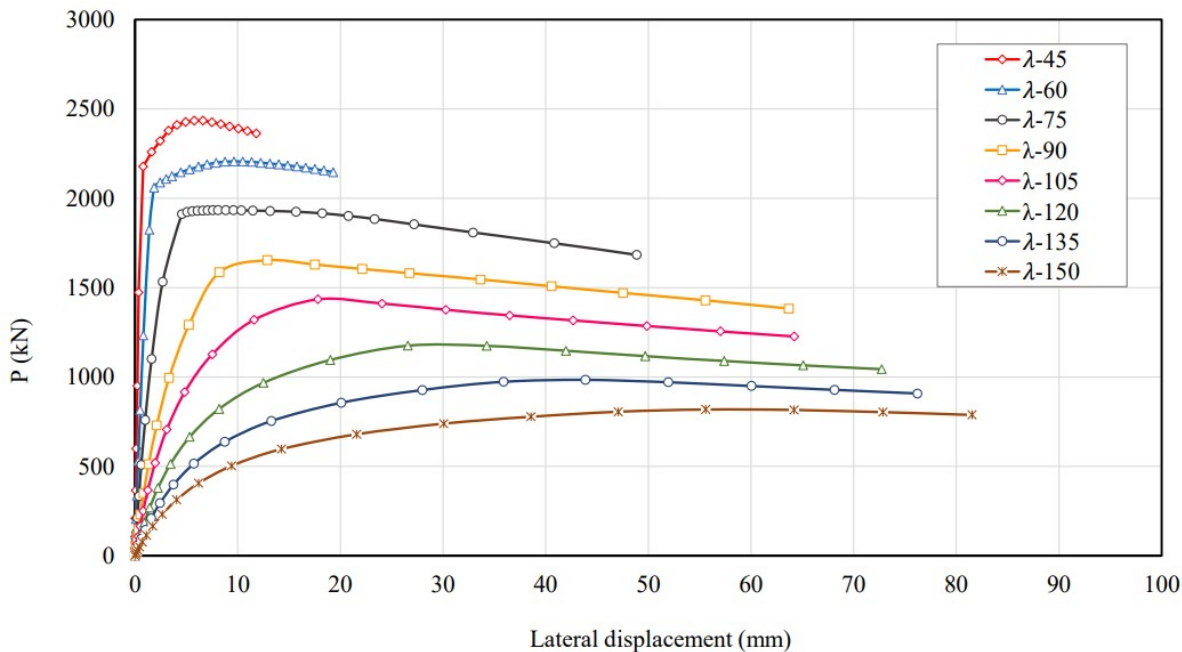


Figure 7. Load-displacement relation for models with geometric imperfection of L/1000 and residual stress of 30% of  $\sigma_y$

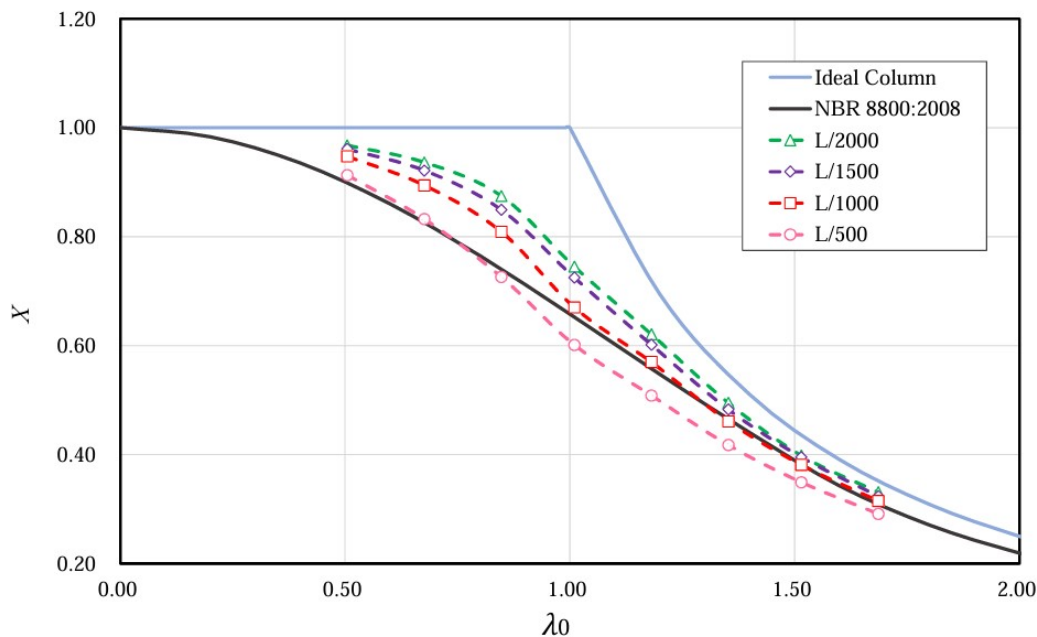


Figure 8. Column curve to different values of initial geometric imperfection

The Fig. 9 illustrates the column curve for an initial geometric imperfection of L/1000, combined with different values of residual stresses (5%, 10%, 20% and 30% of  $\sigma_y$ ) applied to each model. It is evident that an increase in residual stress reduces the columns final compressive strength. As a result, the lowest critical loads were observed in models with residual stress equal to 30% of  $\sigma_y$ , while the highest critical loads were seen in models free of residual stresses. Additionally, the models with residual stress ranging from 10% and 20% of  $\sigma_y$  align most closely with the column curve provided by NBR 8800:2008.

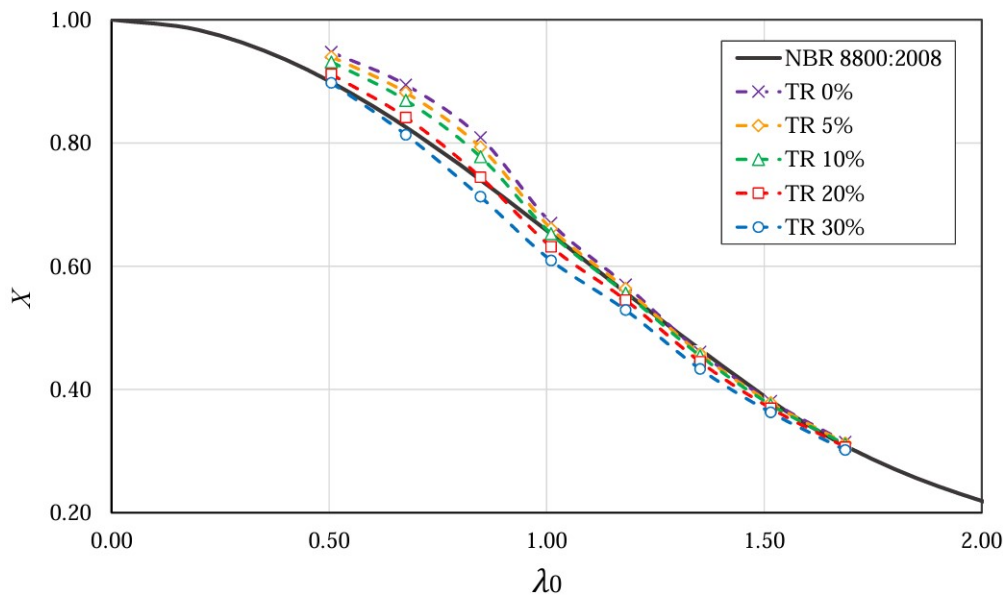


Figure 9. Column curve to an initial geometric imperfection of  $L/1000$  and different values of residual stresses

## 4 Conclusions

The present study showed that the presence of geometric imperfections and residual stresses significantly reduces the columns final compressive strength, emphasizing the importance of considering them during the design phase. The numerical analysis confirms that the column curve provided by NBR 8800:2008 accounts for these effects. The models with an initial geometric imperfection of  $L/1000$  and residual stress ranging from 10% and 20% of  $\sigma_y$  showed column curves closely aligned with those specified by the standard. Therefore, despite variations in the distribution and intensity of residual stresses across structures, the column curve established by NBR 8800:2008 is capable of providing consistent results within the established safety limits.

Thus, the finite element approach presented in this work accurately simulated the structural behavior of steel columns. This enabled comprehensive analyses encompassing both elastic and nonlinear behaviors, providing insights into the effects of initial geometric imperfections and residual stresses.

**Acknowledgements.** The authors gratefully acknowledge the financial support provided by the Coordenação de Aperfeiçoamento de Pessoal de Nível Superior - Brasil (CAPES) - Finance Code 001 and Conselho Nacional de Desenvolvimento Científico e Tecnológico (CNPq).

**Authorship statement.** The authors hereby confirm that they are the sole liable persons responsible for the authorship of this work, and that all material that has been herein included as part of the present paper is either the property (and authorship) of the authors, or has the permission of the owners to be included here.

## References

- [1] L. C. Mesquita, A. F. F. Gomes, and F. S. Leão. Simulação computacional de pilares de aço submetidos à compressão axial. *REEC-Revista Eletrônica de Engenharia Civil*, vol. 15, n. 2, pp. 203–216, 2019.
- [2] T. V. Galambos and A. E. Surovek. *Structural stability of steel: concepts and applications for structural engineers*. John Wiley & Sons, 2008.
- [3] ABNT NBR 8800: Projeto de estruturas de aço e de estruturas mistas de aço e concreto de edifícios. Rio de Janeiro: ABNT, 2008.
- [4] Z. P. Bazant, L. Cedolin, and J. Hutchinson. *Stability of structures: elastic, inelastic, fracture, and damage theories*. World Scientific, 2010.
- [5] A. Chajes. *Principles of structural stability theory*. Prentice Hall, 1974.
- [6] A. C. B. Almeida and A. C. C. Lavall. Influência das tensões residuais na resistência de pilares de aço considerando a análise avançada com plasticidade distribuída. *Rem: Revista Escola de Minas*, vol. 60, n. 2, pp. 391–399, 2007.